HHS Public Access

Author manuscript

ACS Appl Mater Interfaces. Author manuscript; available in PMC 2016 August 12.

Published in final edited form as:

ACS Appl Mater Interfaces. 2015 August 12; 7(31): 17535–17544. doi:10.1021/acsami.5b05497.

Lipopeptide-Coated Iron Oxide Nanoparticles as Potential Glycoconjugate-Based Synthetic Anticancer Vaccines

Suttipun Sungsuwan, **Zhaojun Yin**, and **Xuefei Huang***

Department of Chemistry, Michigan State University, Chemistry Building, Room 426, 578 South Shaw Lane, East Lansing, Michigan 48824, United States

Abstract

Although iron oxide magnetic nanoparticles (NPs) have been widely utilized in molecular imaging and drug delivery studies, they have not been evaluated as carriers for glycoconjugate-based anticancer vaccines. Tumor-associated carbohydrate antigens (TACAs) are attractive targets for the development of anticancer vaccines. Due to the weak immunogenicity of these antigens, it is highly challenging to elicit strong anti-TACA immune responses. With their high biocompatibilities and large surface areas, magnetic NPs were synthesized for TACA delivery. The magnetic NPs were coated with phospholipid-functionalized TACA glycopeptides through hydrophobic–hydrophobic interactions without the need for any covalent linkages. Multiple copies of glycopeptides were presented on NPs, potentially leading to enhanced interactions with antibody-secreting B cells through multivalent binding. Mice immunized with the NPs generated strong antibody responses, and the glycopeptide structures important for high antibody titers were identified. The antibodies produced were capable of recognizing both mouse and human tumor cells expressing the glycopeptide, resulting in tumor cell death through complement-mediated cytotoxicities. These results demonstrate that magnetic NPs can be a new and simple platform for multivalently displaying TACA and boosting anti-TACA immune responses without the need for a typical protein carrier.

*Corresponding Author: xuefei@chemistry.msu.edu.

Supporting Information: The Supporting Information is available free of charge on the ACS Publications website at DOI: 10.1021/acsami.5b05497.

Material and instrumentation, synthesis and characterization of Tn antigen, lipo(glyco)peptides, synthesis and characterization of nanoparticles, biological experiments, and additional supporting data (PDF).

Notes: The authors declare no competing financial interest.

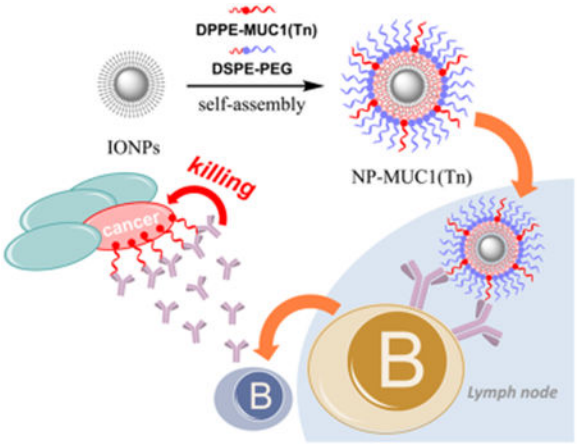

Keywords

cancer vaccine; glycopeptide; immunology; MUC1; magnetic nanoparticles

1. Introduction

The development of vaccine constructs to elicit effective immune responses against cancer cells is of high current interest.[1] Among many tumor -associated antigens, glycans, including glycolipids and glycopeptides, are attractive targets for anticancer vaccines due to their wide expression on multiple types of tumor cells and their importance in tumor development.[2–8] As tumor-associated carbohydrate antigens (TACAs) are self-antigens, they are weakly immunogenic. Commonly, protein carriers such as keyhole limpet hemocyanin[9,10] and tetanus toxoid[11,12] have been utilized to deliver TACAs to the immune system and to boost immune responses. One limitation with these carriers is that the high anticarrier responses[13] can compete with the desired anti-TACA immunity.[14,15] Furthermore, as the host can have high titers of anticarrier antibodies due to prior immunization, the preexisting anticarrier antibodies can pose severe interference against antiglycan immunity.[16,17] Therefore, new delivery platforms are needed to complement the existing carriers.

Recently, nanotechnology has seen tremendous growth in glycoscience applications.[18,19] Superparamagnetic Fe_3O_4 NPs are an important class of inorganic NPs.[20,21] Although glycancoated magnetic NPs have been utilized for imaging, drug delivery, and immune activation,[18,19,22] they have not been evaluated as potential TACA-based anticancer vaccines. Magnetic NPs are highly biocompatible and have been approved by the FDA for use as contrast agents in humans.[23] Due to their large surface area, multiple copies of an antigen can be displayed on the NPs' surface, which can lead to enhanced affinity with antibody-secreting B cells through multivalent interactions, boosting humoral responses.[24] Magnetic NPs can be efficiently internalized by dendritic cells with no observed toxicities.[25,26] Furthermore, with their magnetic properties, magnetic NPs can be functionalized for use as magnetic resonance imaging (MRI) contrast agent.[23,27–30] This can

enable *in vivo* tracking and monitoring of labeled DCs by MRI following vaccine administration, which could shine light on the mechanism of immune activation.[31,32]

Herein, we report results aimed at establishing magnetic NPs as an effective system to deliver TACAs to the immune system, with the mucin-1 (MUC1) glycopeptide as a representative antigen. MUC1 is a transmembrane glycoprotein bearing multiple glycosylations at serine or threonine residues (referred to as O-glycosylation) on a variable number of 20 amino acid tandem repeats.[33] MUC1 is overexpressed on many types of cancer cells, including ovarian, prostate, and breast cancer cells, and its expression levels can be correlated with tumor progression and metastasis.[34,35] In addition to its high expression levels, cancer-associated MUC1 typically bears short O-linked glycans such as Tn (*N*-acetylgalactosamine linked with serine or threonine), presenting it as an attractive target for anticancer vaccine development. We synthesized amphiphilic MUC1 lipo(glyco)peptides, which could readily self-assemble onto magnetic NPs for antigen presentation to the immune system. The MUC1 NPs were able to induce the production of MUC1-specific antibodies, which recognized MUC1-positive tumor cells and killed tumor cells through complement-mediated cytotoxicity.

2. Results

2.1. Synthesis of Magnetic NPs Coated with MUC1 Lipopeptides and Lipo-Glycopeptides

We utilized the thermal decomposition method[36] to prepare high-quality monodisperse iron oxide nanocrystals on a large scale and with excellent control of the particle diameter. Homogeneity in size is important in NP-based vaccine design, as the diameter of NPs can significantly impact their interactions with the immune system as well as their trafficking.[37,38] Covalent derivatization of NPs can be tedious. NPs synthesized through the thermal decomposition method are coated with a hydrophobic layer of oleic acid or oleic amine. This provides a platform for amphiphilic TACA to self-assemble on the NPs through hydrophobic–hydrophobic interactions without the need to covalently functionalize the NPs. This approach is operationally simple, and an additional advantage is that multiple components can be readily introduced onto the NPs through self-assembly to boost the immune responses.

In order to attach MUC1 onto the NPs, MUC1 peptide and glycopeptide were synthesized and conjugated with a phospholipid chain. The MUC1 peptide bearing 20 amino acid residues, AHGVTSAPDTRPAPGSTAPP, corresponding to one full-length tandem repeat region, was produced using solid-phase peptide synthesis through Fmoc chemistry, using 2-chlorotrityl resin as a solid support and *O*-(benzotriazol-1-yl)-*N*,*N*,*N*′,*N*′-tetramethyluronium hexafluorophosphate (HBTU) and 1-hydroxybenzotriazole (HOBt) as coupling agents (Scheme 1). Upon completion of the synthesis, MUC1 peptide **1** was cleaved off the solid phase under an acidic condition (95:2.5:2.5, TFA/TIPS/H_2O) and purified by HPLC on a C18 reverse-phase column. In order to conjugate the peptide with the lipid chain, phosphatidylethanolamine was treated with succinic anhydride to introduce a carboxylic group to the lipid part. The carboxylic group was then activated with *N*,*N*,*N*′,*N*′-tetramethyl-*O*-(*N*-succinimidyl)uronium tetrafluoroborate (TSTU) to form an NHS ester (**DPPE-SUC-**

NHS). **DPPE-SUC-NHS** was incubated with MUC1 peptide **1**, producing lipopeptide **5**, which was purified through HPLC on a reverse-phase C4 column.

In addition to unglycosylated MUC1 peptide **5**, three MUC1 lipo-glycopeptides **6–8** were synthesized using Tn-substituted threonine (**Fmoc-*p*Tn-Thr-OH**) (see Supporting Information S1 for synthetic procedures) to replace the corresponding threonine building block in solid-phase peptide synthesis (Scheme 1). Lipo-glycopeptide **6** contains a Tn antigen in the PDT*R region only, and lipo-glycopeptide **7** bears Tn as part of the GST*A sequence, whereas lipo-glycopeptide **8** has Tn in both locations. 1-[Bis(dimethylamino)methylene]-1*H*-1,2,3-triazolo[4,5-*b*]pyridinium 3-oxid hexafluorophosphate (HATU) and 1-hydroxy-7-azabenzotriazole (HOAT) were used as coupling agents for adding **Fmoc-*p*Tn-Thr-OH** to the peptide chain. After being released from the resin, glycopeptides **6–8** were obtained by deprotection with 5% (v/v) hydrazine hydrate followed by HPLC purification. These lipo(glyco)peptides are useful to probe the impact of the number and location of Tn on immune responses.

With the lipopeptides in hand, antigen-coated magnetic NPs were prepared. The oleic acid-coated iron oxide NPs (OA-IONPs) were obtained by thermal decomposition of iron(III) acetylacetonate ($Fe(acac)_3$) in the presence of oleic acid and oleylamine at an elevated temperature (Figure 1).[39] The OA-IONPs produced have a mean size of 9 nm and a narrow polydispersity index (PDI) of 0.079 when measured as a solution in chloroform. The highly hydrophobic surface of the OA-IONPs rendered them insoluble in water. To facilitate changes in the surface polarity and to reduce NP aggregation in water, a dual solvent exchange method[40] was utilized for antigen coating (Figure 1). A mixture of the lipopeptide (DPPE-MUC1) and lipopolymer (DSPE-PEG2000) was added to a solution of OA-IONPs in chloroform. This was followed by slow addition of DMSO. Chloroform was then slowly evaporated under vacuum to induce the assembly of the amphiphilic DPPE-MUC1 and DSPE-PEG on NPs. Subsequently, DMSO was replaced with water through dialysis. Using this procedure, the solvent polarity gradually increased to strengthen the hydrophobic interactions and assemble the lipopeptide and lipo-glycopeptide onto the NP. The NPs produced were well-dispersed in water. The control particle, NP-PEG without any (glyco)peptide (**NP-9**), was also prepared using a DSPE-PEG2000 coating only.

The magnetic NPs were characterized. Dynamic light scattering (DLS) indicated that the hydrodynamic diameters in water were around 35 nm (Table 1 and Figure S4). The incorporation of the glycopeptides slightly increased the size of the coated NPs compared with that of the control **NP-9** with PEG only. The zeta potentials of all NPs are slightly negative, presumably due to the phosphate groups present.

To ascertain the successful immobilization of the lipopeptides, the NPs were subjected to mass spectrometry (MS) analysis. Since lipopeptides were attached through noncovalent interactions, the coating of the NP could be readily ionized by matrix-assisted laser desorption ionization (MALDI). The MALDI-TOF mass spectrum of **NP-5** showed the desired *m*/*z* ratio of lipopeptide **5** (MW = 2661), which was not found in the spectrum of **NP-9** coated with DSPE-PEG only (Figures 2a and S5 for **NP-6**, **NP-7**, and **NP-8**). For lipopeptide quantification, the NPs were loaded onto a SDS-PAGE gel for electrophoresis,

which was then visualized through silver staining (Figure 2b). The intensities of the bands were compared with a calibration curve generated based on bands from known amounts of free lipopeptides. From this analysis, it was determined that there was an average of 23 molecules of MUC1 per NP (Supporting Information S4–4).

2.2. *In Vitro* Activation of Dendritic Cells and Detection of NP Draining into Local Lymph Nodes *in Vivo*

Dendritic cells are important antigen-presenting cells that modulate immune responses.[41] To test DC interactions, **NP-9** was incubated with bone-marrow derived dendritic cells (BMDCs). The NPs do not directly induce maturation of DCs, as the expression levels of costimulatory molecules and activation markers on dendritic cells were unchanged upon NP incubation, suggesting good biocompatibility of the NPs (Figure 3a).

The immune-potentiating activities of the NP construct can be bestowed by adding an agonist of Toll-like receptor 4 (TLR4), monophospholipid A (MPLA).[42] MPLA can elicit T cell responses and antibody isotype class switching from IgM to IgG.[43] With its amphiphilic nature, MPLA could also be immobilized onto the NPs through hydrophobic interactions.[44] The addition of MPLA to **NP-9** led to an enhancement of the expression of costimulatory molecules, such as CD40, CD80, CD86, and MHC class II on DCs, as indicated by FACS analysis (Figure 3a). The expression of these costimulatory molecules on APCs are crucial for activation of the immune system. To confirm NP interactions with cells, **NP-9** was labeled with a fluorophore, fluorescein isothiocyanate (FITC). Upon incubation with BMDCs, fluorescence microscopy showed extensive green fluorescence inside the cells, indicating NP uptake (Figures 3b vs 3c). Similar NP uptake by BMDCs was observed with or without MPLA (Figure S8).

An important feature of our NP is that their hydrodynamic diameters are around 35 nm, which is within the size range required for their ready trafficking to lymph nodes for interactions with resident immunological cells.[38] To test transport to lymph nodes, NPs were injected subcutaneously into mice under their scruff. After 24 h, mice were sacrificed, and their lymph nodes were removed and stained with Prussian blue, a dye sensitive to the presence of ferric ions. Histological analysis showed that the axillary (local) lymph nodes close to the injection sites exhibited extensive blue color in the B cell follicle region (Figure 3d), whereas there was much less blue staining in the inguinal (distant) lymph node (Figure 3e). This result suggested that the NPs could drain into local lymph nodes to interact with immunological cells.

2.3. Immunization with MUC1-Coated NPs Elicited Strong Anti-MUC1 IgG Responses

To evaluate the ability of the NP vaccines to induce an immune response *in vivo*, mice were injected with NP-MUC1 (**NP-5**, **NP-6**, **NP-7**, **NP-8**) (corresponding to 20 μg of MUC1 peptide or glycopeptide) mixed with MPLA. Booster injections were performed on days 14 and 28. To decipher the importance of various vaccine components, control groups of mice received NP-PEG (**NP-9**)/MPLA, MUC1 peptide **1**/MPLA, or MUC1 lipopeptide **5**/MPLA at the same doses of NP and MUC1, respectively. Sera were collected from all mice a week after the final immunization.

The levels of antibody elicited were analyzed by enzyme-linked immunosorbent assay (ELISA) using plates coated with the corresponding MUC1 or MUC1(Tn) glycopeptide. Mice (n = 5) immunized with MUC1 NP vaccines elicited both IgG and IgM antibodies (Figure 4a,c), with higher IgG titers. In contrast, MUC1 peptide **1** failed to generate any appreciable amounts of anti-MUC1 antibodies. Interestingly, immunization with MUC1 lipopeptide **5** produced some anti-MUC1 IgG antibodies (mean titer ∼5032), although the titers were significantly lower than those induced by **NP-5** (mean IgG titer ∼36 603, Figure 4a). The ability of lipopeptide MUC1 to generate antibodies may be due to the effect of lipid rendering MUC1 amphiphilic. The endogenous mouse serum albumin could absorb the amphiphilic lipopeptide and deliver the antigen into the lymph node for B cell activation.[45] The higher potency of the MUC1 NP construct to induce antibodies could be partly attributed to the efficient trafficking of NPs into the lymph nodes due to the suitable size regime of the NPs.[38] In addition, the NPs can present the glycopeptides in a multivalent manner, rendering them more efficient at cross-linking B-cell receptors and eliciting potent cellular activation.[24]

The availability of NPs bearing various MUC1 glycoforms enabled us to investigate the effects of glycosylation on antibody titers. PDT*R-MUC1 **NP-6** gave the highest IgG titers (mean titers ∼81 402) compared to those with GST*A-MUC1 **NP-7** (mean titers ∼45 526) and unglycosylated MUC1 **NP-5** (mean titers ∼36 603) (Figure 4a). Interestingly, diglycosylated MUC1 **NP-8** gave significantly lower IgG titers (mean titers ∼7530) than those with **NP-6** and **NP-7**.

The anticarrier responses were tested next. ELISA analysis showed that significantly lower titers (∼200) of antibodies were generated against the NP carrier by **NP-5** than those against MUC1 (Figure 4b). This suggests that the immune responses were primarily focused on MUC1.

The subtypes and cross-recognition of IgG antibodies elicited against MUC1 were analyzed. Higher levels of IgG2b over IgG1 were observed in all MUC1-vaccinated groups (Figure 4d), which suggested a type 1 T helper cell (T_H1)-skewed immune response and the generation of cell-mediated immunity.[46,47] The elicited antibodies from mice immunized with all NP vaccines could recognize other Tn-MUC1 glycopeptides (Figure S9).

2.4. Antibodies from Immunized Mice Showed Binding- and Complement-Dependent Cytotoxicity against MUC1-Expressing Tumor Cells

Because ELISA tests binding to synthetic MUC1 (glyco)peptides, it is important that antibodies generated can recognize MUC1 on cancer cells. This was first tested with MUC1-transfected Ag104 cells, which express MUC1 containing exclusively Tn due to the dysfunction of Cosmc, a molecular chaperone.[48,49]

MUC1-Ag104 cells were incubated with sera from immunized mice followed by FITC-labeled anti-mouse IgG secondary antibody. FACS analysis of the tumor cells indicated that the serum from mice immunized with MUC1 peptide **1** did not bind to the cells very much (Figure 5a). In contrast, the MUC1 NPs induced antibodies capable of recognizing MUC1-Ag104 strongly. The recognition was MUC1-dependent, as antibody binding to MUC1-

Ag104 was much stronger than that to Ag104 cells without MUC1 transfection (Supporting Information, Figure S10a). Moreover, the induced antibodies showed high selectivity toward MUC1-Ag104 with little binding to normal epithelial cells (Supporting Information, Figure S10b). Consistent with the ELISA results, sera from mice immunized MUC1 **NP-6** exhibited the strongest binding with MUC1-Ag104 cells. When these cells were incubated with the rabbit complement as well as the sera from MUC1 NP immunized mice, the majority of cancer cells were killed, suggesting that the anti-MUC1 antibodies induced complement-dependent cytotoxicity to the cancer cells (Figure 5b).

Next, the interactions of postimmune sera with MCF-7 human breast cancer cells were studied. MCF-7 naturally expresses MUC1 on the cell surface. Antibodies elicited by MUC1 NP vaccines were also capable of binding MCF-7 cells (Figure 5c). The binding of antibodies from mice immunized with **NP-6** and **NP-7** showed similar affinities and was higher than those immunized with unglycosylated MUC1 **NP-5** and di-Tn MUC1 **NP-8** vaccines. The MUC1 NP vaccines were also capable of inducing complement-dependent cytotoxicity against MCF-7 (Figure 5d).

3. Discussion

While magentic NPs have seen wide biomedical applications, they have not been utilized as TACA carriers in vaccine development. With the MUC1-magentic NP vaccines, significantly higher IgG antibody responses were observed compared to those of mice immunized with MUC1 peptide or lipopeptide. A study from Hubbell and co-workers[38] emphasized the crucial effect of size for vaccines. NPs with a 25 nm diameter can target lymph node-residing dendritic cells, which are more efficient in immune activation than dendritic cells in skin, but 100 nm NPs are less likely to drain into the lymph nodes. The size of our NPs (30–40 nm) is likely a contributing factor to the observed high antibody responses. The fact that anti-MUC1 IgG antibodies were induced suggests that magnetic NP vaccines can activate helper T cells and elicit antibody isotype switching without the need for a traditional immunogenic protein carrier or additional helper T cell epitopes. Furthermore, the magnetic NP itself is almost nonimmunogenic, inducing a low amount of anticarrier antibodies. These attributes combined suggest that magnetic NPs can be a useful platform for glycoconjugate-based anticancer vaccines, joining other types of NP such as gold NPs, polymer NPs, and virus-like particles[22,50–54]

Compared to MUC1 expressed on normal cells, MUC1 on cancer cells bears shortened O-glycans, as represented by the Tn antigen. Glycosylation of MUC1 leads to conformational changes of the peptide.[55–57] As a result, MUC1 glycopeptides become more immunogenic.[35,58] This is supported by our results that lipo-glycopeptide-coated NPs induced higher antibody titers and stronger binding with MUC1-positive tumor cells than that of unglycosylated MUC1-coated **NP-5**.

As each of the tandem repeats of a MUC1 protein contains five potential glycosylation sites, and MUC1 proteins on tumor cells are hetereogenously glycosylated. Determining how the glycan structure influences humoral responses is an active area of research.[59–65] Within our NP constructs, addition of Tn onto the peptide sequence PDTR showed higher antibody

responses than that with Tn on the GSTA sequence. This suggests that glycosylation in the PDTR region more potently boosted the humoral response in our NP constructs.[47,65] On the other hand, further increasing the number of glycans on the protein may not lead to improved antibody titers, as indicated from the reduced anti-MUC1 titers elicited by **NP-8** bearing two Tns. So far, it is still unclear as to whether full glycosylation on MUC1 enhances the immunogenicity of the vaccine.[66] Our results can provide guidance for selecting glycopeptide structures for future MUC1-based vaccine studies.

MUC1-Ag104 cancer cells exclusively express Tn rather than longer O-glycans.[48,49] As a result, its MUC1 proteins are expected to be solely glycosylated with Tn. The antibodies from immunized mice bound more strongly and exhibited higher cytotoxicity with MUC1-Ag104 as compared to heterogenously glycosylated MCF-7 cells.[63,67] This suggests that a potential approach to improve the recognition of MCF-7 cells is to incorporate MUC1 glycopeptides bearing multiple types of glycan structures.

4. Conclusions

Iron oxide magnetic NPs were investigated as a new antigen carrier platform for a MUC1-based cancer vaccine. A simple procedure was developed to immobilize lipo(glyco)peptides onto the NPs through self-assembly without the need for covalent NP functionalization. MUC1-specific IgG antibody responses were produced. Besides MUC1, this strategy can be readily applied to vaccines targeting other glycopeptides. In addition, glycolipids such as gangliosides are another class of important TACAs. The magnetic NP approach can be potentially useful for vaccines targeting amphiphilic glycolipids as well.

With the large surface area of the NPs, multiple lipopeptides were incorporated. The resulting lipopeptide NPs could drain into local lymph nodes of mice upon vaccination and activate the immune sytem to elicit the production of MUC1-specific antibodies. Compared to the antigen in soluble forms, the nanovaccine induced higher antibody titers, presumbly due to the suitable sizes of the NPs and the multivalent display of antigens on the particles' surface. Combined with the low antibody titers against the carrier, this highlights the advantages of the magentic NP platform.

Immunological evaluations of MUC1 NPs demonstrated that the number and position of Tn in the glycopeptide chain can impact antibody titers. A single Tn in the PDTR region gave the highest anti-MUC1 IgG titers. The antibodies generated not only selectively recognized MUC1-expressing tumor cells but also mediated complement-dependent cytotoxicity for tumor cell killing. Therefore, the magnetic NPs represent a new and effective platform for the development of TACA-based synthetic anticancer vaccines.

5. Experimental Section

5.1. Synthesis of MUC1 1 and Tn-MUC1 2–4

The MUC1 lipopeptide was derived from the conjugation of phospholipid (**DSPE-SUC-NHS**) and the tandem repeat MUC1 peptide. The MUC1 peptide was synthesized using Fmoc-chemistry-based solid-phase support peptide synthesis, starting from a 2-chlorotrityl resin preloaded with Fmoc-proline. The N-terminal protecting group, Fmoc-, was

deprotected by 20% piperidine in DMF. The amino acid coupling was carried out with Fmoc amino acids (5 equiv) using HBTU/HOBt (4.9 equiv) and DIPEA (10 equiv) or with Fmoc-Tn building block **Fmoc-*p*Tn-Thr-OH** (2 equiv) using HATU/HOAT (1.9 equiv) and DIPEA (4 equiv). The peptide was cleaved from resin by TFA/TIS/H_2O = 95:2.5:2.5 for 30 min. Excess TFA was evaporated off, and the peptide was precipitated by diethyl ether and centrifuged to pellet the precipitate. The peptide was further reprecipitated three times. To remove the acetyl protecting group of Tn, the crude peptide was treated with 5% (v/v) hydrazine acetate for 2 h. The crude reaction was neutralized to pH 7. The deprotected peptide was then purified by HPLC, using a reverse-phase column, SUPERCOSIL LC18, 25 cm × 10 mm 5 μm, with a solvent gradient of CH_3CN and H_2O (0.1% TFA) of 0–22% in 25 min and 100% in 10 min. The product was identified by MALDI-TOF.

5.2. Synthesis of Lipo-(Tn)-peptide (DPPE-MUC1 5 and DPPE-Tn-MUC1 6–8)

The phospholipid was linked to succinic acid linker by reaction of DPPE with succinic anhydride and 2 equiv of Et_3N. The carboxylic acid group of the succinic linker was then activated by TSTU (*N*,*N*,*N*′,*N*′-tetramethyl-*O*-(*N*-succinimidyl)uranium tetrafluoroborate) to provide compound **DSPE-SUC-NHS**. The activated phospholipid was coupled to the N-terminus of purified (glyco)peptides **1–4**. The lipopeptide was purified by HPLC, using a C_4-column (Kromasil; 5 μm, 4.6 × 150 mm 5 μm; part no. PSL847277), with a gradient of 30% isopropanol in H_2O (0.1% TFA) to 100% in 40 min.

5.3. Preparation of Iron Oxide NPs (OA-IONPs)

A mixture of iron(III) acetylacetonate [$Fe(acac)_3$], 1,2-hexadecanediol, oleic acid, and oleyl amine in benzyl ether was stirred under a flow of nitrogen. The mixture was heated at 200 °C for 2 h, followed by refluxing (300 °C) for 1 h. The black mixture was allowed to cool to room temperature, and excess starting materials were washed out by adding ethanol into the mixture followed by external magnetic separation. The iron oxide NPs dispersed in toluene were centrifuged at 6000 rpm to further remove the large particulates, and the supernatant containing **OA-IONPs** was collected (5 mg/mL).

5.4. Preparation of NP5–9

The lipopolymer (DSPE-PEG, 2 mg) dispersed in 100 μL of chloroform was mixed with **OA-IONPs** (1 mg), which were predissolved in THF. The lipopeptide or lipoglycopeptide (1 mg) dissolved in DMSO (50 μL) was added into the mixture. DMSO (4 mL) was slowly added into the mixture while shaking. The incubated mixture was left to sonicate for 30 min; then, all low boiling point solvents, chloroform and THF, were completely evaporated under vacuum for 2 h. Water (20 mL) was slowly added into the vial while shaking. DMSO and excess starting materials were removed by centrifugal filtration (100 kDa cutoff) and washed with water five times. The solution of NPs was finally filtered through a 0.22 μm filter to remove any large particles. NPs coated only with lipopolymer (NP-PEG, **NP-9**), used as a control, were synthesized by the same procedure. For NP-PEG-FITC used in dendritic cell uptake experiment, the NPs were coated using the same procedure as that for NP-PEG but DSPE-PEG(2000)-NH_2 was used instead. The coated NPs were subsequently

reacted with FITC in water. The excess FITC was washed extensively by centrifugal filtration (100 kDa cutoff). The FITC-conjugated NPs were then resuspended in PBS.

5.5. Mouse Immunization

Pathogen-free female mice age 7–9 weeks were obtained from breeding and cared for in the University Laboratory Animal Resources facility of Michigan State University. All animal care procedures and experimental protocols have been approved by the Institutional Animal Care and Use Committee (IACUC) of Michigan State University. Mice (5 mice each group) were immunized subcutaneously under their scruff with NPs or soluble vaccine in 100 μL of PBS on days 0, 14, and 28. Serum samples were collected on days 0 (before immunization) and 35.

5.6. Elisa

A 96-well Nunc microtiter plate was coated with 100 μL/well of 10 μg/mL purified MUC1 or glyco MUC1 peptides in 0.05 M carbonate buffer (pH 9.6) and incubated at 4 °C overnight. The plate was then washed four times with PBS/0.5% Tween-20 (PBST), followed by blocking with 1% (v/v) BSA in PBS at room temperature for 1 h. Subsequently, the plates were washed four times with PBST. Then, the plates were incubated with 100 μL of diluted mouse antisera in 0.1% BSA/PBS at 37 °C for 2 h, followed by washing four times with PBST. Bound antibodies were detected with 1:2000 diluted horseradish peroxidase (HRP) conjugated goat anti-mouse IgG, IgG1, IgG2b, IgG2c, or IgG3 at 37 °C for 1 h, followed by washing four times with PBST. Then, plates were incubated with TMB substrate for 15 min. The reaction was stopped with 2 M H_2SO_4 (50 μL), and the absorbance was measured at 450 nm using a microplate autoreader (BioRad). The titer was determined by regression analysis with $\log_{10}$ dilution plotted with optical density. The titer was calculated as the highest dilution that gave OD = 0.3.

5.7. Complement-Dependent Cytotoxicity

Complement-dependent cytotoxicity of MUC1-Ag104 and MCF-7 tumor cells was determined by MTS assay. MUC1-Ag104 or MCF-7 cells (7000 cells/well) were incubated on ice with a $^1/_{20}$ dilution of antisera in 100μL of PBS from different groups of immunized mice. After removing the unbound antisera through washing, rabbit sera at a $^1/_5$ dilution in100 μL of culture medium were added and then incubated at 37 °C for 8 h. MTS (CellTiter 96 AQueous One Solution Cell Proliferation Assay; Promega, 20 μL) was added into each well and further incubated at 37 °C for 4 h. The optical absorption of the MTS assay was measured at 490 nm. Cells cultured in medium alone were used as a positive control (maximum OD), and culture medium was used as a negative control (minimum OD). All data were performed with four repeats. Cytotoxicity was calculated as follows: cytotoxicity (%) = (OD positive control – OD experimental)/(OD positive control – OD negative control) × 100.

Supplementary Material

Refer to Web version on PubMed Central for supplementary material.

Acknowledgments

We are grateful to the National Cancer Institute (R01CA149451-01A1) for financial support of our work.

References

1. Melero I, Gaudernack G, Gerritsen W, Huber C, Parmiani G, Scholl S, Thatcher N, Wagstaff J, Zielinski C, Faulkner I, Mellstedt H. Therapeutic Vaccines for Cancer: An Overview of Clinical Trials. Nat Rev Clin Oncol. 2014; 11:509–524. [PubMed: 25001465]
2. Livingston PO, Zhang S, Lloyd KO. Carbohydrate Vaccines That Induce Antibodies Against Cancer. 1. Rationale. Cancer Immunol Immunother. 1997; 45:1–9. [PubMed: 9353421]
3. Buskas T, Thompson P, Boons GJ. Immunotherapy for Cancer: Synthetic Carbohydrate-Based Vaccines. Chem Commun. 2009:5335–5349.
4. Cazet A, Julien S, Bobowski M, Burchell J, Delannoy P. Tumour-Associated Carbohydrate Antigens in Breast Cancer. Breast Cancer Res. 2010; 12:204. [PubMed: 20550729]
5. Guo ZW, Wang QL. Recent Development in Carbohydrate-Based Cancer Vaccines. Curr Opin Chem Biol. 2009; 13:608–617. [PubMed: 19766052]
6. Liu CC, Ye XS. Carbohydrate-based Cancer Vaccines: Target Cancer with Sugar Bullets. Glycoconjugate J. 2012; 29:259–271.
7. Yin Z, Huang X. Recent Development in Carbohydrate Based Anticancer Vaccines. J Carbohydr Chem. 2012; 31:143–186. and references cited therein. [PubMed: 22468019]
8. Monzavi-Karbassi B, Pashov A, Kieber-Emmons T. Tumor-Associated Glycans and Immune Surveillance. Vaccines. 2013; 1:174–203. [PubMed: 26343966]
9. Danishefsky SJ, Allen JR. From the Laboratory to the Clinic: A Retrospective on Fully Synthetic Carbohydrate-Based Anticancer Vaccines. Angew Chem, Int Ed. 2000; 39:836–863.
10. Sabbatini, Pj; Ragupathi, G.; Hood, C.; Aghajanian, CA.; Juretzka, M.; Iasonos, A.; Hensley, ML.; Spassova, MK.; Ouerfelli, O.; Spriggs, DR.; Tew, WP.; Konner, J.; Clausen, H.; Abu Rustum, N.; Dansihefsky, SJ.; Livingston, PO. Pilot Study of A Heptavalent Vaccine-Keyhole Limpet Hemocyanin Conjugate Plus QS21 in Patients with Epithelial Ovarian, Fallopian Tube, or Peritoneal Cancer. Clin Cancer Res. 2007; 13:4170–4177. [PubMed: 17634545]
11. Hoffmann-Roder A, Kaiser A, Wagner S, Gaidzik N, Kowalczyk D, Westerlind U, Gerlitzki B, Schmitt E, Kunz H. Synthetic Antitumor Vaccines from Tetanus Toxoid Conjugates of MUC1 Glycopeptides with the Thomsen-Friedenreich Antigen and A Fluorine-substituted Analogue. Angew Chem, Int Ed. 2010; 49:8498–8503.
12. Rich JR, Wakarchuk WW, Bundle DR. Chemical and Chemoenzymatic Synthesis of S-linked Ganglioside Analogues and Their Protein Conjugates for Use as Immunogens. Chem - Eur J. 2006; 12:845–858. [PubMed: 16196067]
13. Deng K, Adams MM, Damani P, Livingston PO, Ragupathi G, Gin DY. Synthesis of QS-21-Xylose: Establishment of the Immunopotentiating Activity of Synthetic QS-21 Adjuvant with A Melanoma Vaccine. Angew Chem, Int Ed. 2008; 47:6395–6398.
14. Buskas T, Li Y, Boons GJ. The Immunogenicity of the Tumor-Associated Antigen Lewis^y May Be Suppressed by A Bifunctional Cross-Linker Required for Coupling to A Carrier Protein. Chem - Eur J. 2004; 10:3517–3524. [PubMed: 15252797]
15. Sad S, Gupta HM, Talwar GP, Raghupathy R. Carrier-Induced Suppression of the Antibody Response to a 'Self' Hapten. Immunology. 1991; 74:223–227. [PubMed: 1748470]
16. Herzenberg LA, Tokuhisa T. Epitope-Specific Regulation. I. Carrier-Specific Induction of Suppression for IgG Antihapten Antibody Responses. J Exp Med. 1982; 155:1730–1740. [PubMed: 6176665]
17. Di John D, Wasserman SS, Torres JR, Cortesia MJ, Murillo J, Losonsky GA, Herrington DA, Sturcher D, Levine MM. Effect of Priming with Carrier on Response to Conjugate Vaccine. Lancet. 1989; 334:1415–1418. [PubMed: 2480499]
18. Marradi M, Chiodo F, Garcia I, Penadés S. Glyconano-particles as Multifunctional and Multimodal Carbohydrate Systems. Chem Soc Rev. 2013; 42:4728–4745. [PubMed: 23288339]

19. El-Boubbou K, Huang X. Glyco-Nanomaterials: Translating Insights from the “Sugar-Code” to Biomedical Applications. Curr Med Chem. 2011; 18:2060–2078. [PubMed: 21517769]
20. Gupta AJ, Gupta M. Synthesis and Surface Engineering of Iron Oxide Nanoparticles for Biomedical Applications. Biomaterials. 2005; 26:3995–4021. [PubMed: 15626447]
21. Laurent S, Forge D, Port M, Roch A, Robic C, Vander Elst L, Muller RN. Magnetic Iron Oxide Nanoparticles: Synthesis, Stabilization, Vectorization, Physicochemical Characterizations, and Biological Applications. Chem Rev. 2008; 108:2064–2110. [PubMed: 18543879]
22. Peri F. Clustered Carbohydrates in Synthetic Vaccines. Chem Soc Rev. 2013; 42:4543–4556. [PubMed: 23250562]
23. Tassa C, Shaw Sy, Weissleder R. Dextran-Coated Iron Oxide Nanoparticles: A Versatile Platform for Targeted Molecular Imaging, Molecular Diagnostics, and Therapy. Acc Chem Res. 2011; 44:842–852. [PubMed: 21661727]
24. Bachmann MF, Jennings GT. Vaccine Delivery: A Matter of Size, Geometry, Kinetics and Molecular Patterns. Nat Rev Immunol. 2010; 10:787–796. [PubMed: 20948547]
25. Mou Y, Chen B, Zhang Y, Hou Y, Xie H, Xia G, Tang M, Huang X, Ni Y, Hu Q. Influence of Synthetic Super-paramagnetic Iron Oxide on Dendritic Cells. Int J Nanomed. 2011; 6:1779–1786.
26. Goya GF, Marcos-Campos I, Fernández-Pacheco R, Sáez B, Godino J, Asín L, Lambea J, Tabuenca P, Mayordomo I, Larrad L, Ibarra MR, Tres A. Dendritic Cell Uptake of Iron-based Magnetic Nanoparticles. Cell Biol Int. 2008; 32:1001–1005. [PubMed: 18534870]
27. Qiao R, Yang C, Gao M. Superparamagnetic Iron Oxide Nanoparticles: from Preparations to In Vivo MRI Applications. J Mater Chem. 2009; 19:6274–6293.
28. He H, David A, Chertok B, Cole A, Lee K, Zhang J, Wang J, Huang Y, Yang VC. Magnetic Nanoparticles for Tumor Imaging and Therapy: A So-Called Theranostic System. Pharm Res. 2013; 30:2445–2458. [PubMed: 23344909]
29. Colombo M, Carregal-Romero S, Casula MF, Gutierrez L, Morales MP, Bohm IB, Heverhagen JT, Prosperi D, Parak WJ. Biological Applications of Magnetic Nanoparticles. Chem Soc Rev. 2012; 41:4306–4334. [PubMed: 22481569]
30. Corot C, Robert P, Idee JM, Port M. Recent Advances in Iron Oxide Nanocrystal Technology for Medical Imaging. Adv Drug Delivery Rev. 2006; 58:1471–1504.
31. Kobukai S, Baheza R, Cobb JG, Virostko J, Xie J, Gillman A, Koktysh D, Kerns D, Does M, Gore JC, Pham W. Magnetic Nanoparticles for Imaging Dendritic Cells. Magn Reson Med. 2010; 63:1383–1390. [PubMed: 20432309]
32. Ferguson PM, Slocombe A, Tilley RD, Hermans IF. Using Magnetic Resonance Imaging to Evaluate Dendritic Cell-based Vaccination. PLoS One. 2013; 8:e65318. [PubMed: 23734246]
33. Tang, Ck; Apostolopoulos, V. Strategies Used for MUC1 Immunotherapy: Preclinical Studies. Expert Rev Vaccines. 2008; 7:951–962. and references cited therein. [PubMed: 18767945]
34. Apostolopoulos V, Hu XF, Pouniotis DS, Xing PX. MUC1: A Molecule of Many Talents. Curr Trends Immunol. 2004; 12:629–639.
35. von Mensdorff-Pouilly S, Moreno M, Verheijen RHM. Natural and Induced Humoral Responses to MUC1. Cancers. 2011; 3:3073–3103. [PubMed: 24212946]
36. Park J, An K, Hwang Y, Park JG, Noh HJ, Kim JY, Park JH, Hwang NM, Hyeon T. Ultra-Large-Scale Syntheses of Monodisperse Nanocrystals. Nat Mater. 2004; 3:891–895. [PubMed: 15568032]
37. Dobrovolskaia M, McNeil S. Immunological Properties of Engineered Nanomaterials. Nat Nanotechnol. 2007; 2:469–478. [PubMed: 18654343]
38. Reddy ST, van der Vlies AJ, Simeoni E, Angeli V, Randolph GJ, O'Neil CP, Lee LK, Swartz MA, Hubbell JA. Exploiting Lymphatic Transport and Complement Activation in Nanoparticle Vaccines. Nat Biotechnol. 2007; 25:1159–1164. [PubMed: 17873867]
39. Sun S, Zeng H, Robinson DB, Raoux S, Rice PM, Wang SX, Li G. Monodisperse MFe_2O_4 (M = Fe, Co, Mn) Nanoparticles. J Am Chem Soc. 2004; 126:273–279. [PubMed: 14709092]
40. Tong S, Hou S, Ren B, Zheng Z, Bao G. Self-Assembly of Phospholipid-PEG Coating on Nanoparticles through Dual Solvent Exchange. Nano Lett. 2011; 11:3720–3726. [PubMed: 21793503]

41. Steinman RM. Dendritic Cells: Versatile Controllers of the Immune System. Nat Med. 2007; 13:1155–1159. [PubMed: 17917664]
42. Iwasaki A, Medzhitov R. Toll-Like Receptor Control of the Adaptive Immune Responses. Nat Immunol. 2004; 5:987–995. [PubMed: 15454922]
43. Pihlgren M, Silva AB, Madani R, Giriens V, Waeckerle-Men Y, Fettelschoss A, Hickman DT, Lopez-Deber MP, Ndao DM, Vukicevic M, Buccarello AL, Gafner V, Chuard N, Reis P, Piorkowska K, Pfeifer A, Kundig TM, Muhs A, Johansen P. TLR4- and TRIF-Dependent Stimulation of B Lymphocytes by Peptide Liposomes Enables T Cell–Independent Isotype Switch in Mice. Blood. 2013; 121:85–94. [PubMed: 23144170]
44. Jeong J, Kwon Ek, Cheong TC, Park H, Cho NH, Kim W. Synthesis of Multifunctional Fe3O4–CdSe/ZnS Nanoclusters Coated with Lipid A Toward Dendritic Cell-based Immunotherapy. ACS Appl Mater Interfaces. 2014; 6:5297–5307. [PubMed: 24641174]
45. Liu H, Moynihan KD, Zheng Y, Szeto GL, Li AV, Huang B, Van Egeren DS, Park C, Irvine DJ. Structure-based Programming of Lymph-Node Targeting in Molecular Vaccines. Nature. 2014; 507:519–522. [PubMed: 24531764]
46. Steinhagen F, Kinjo T, Bode C, Klinman DM. TLR-based Immune Adjuvants. Vaccine. 2011; 29:3341–3355. [PubMed: 20713100]
47. Huang ZH, Shi L, Ma JW, Sun ZY, Cai H, Chen YX, Zhao YF, Li YM. A Totally Synthetic, Self-Assembling, Adjuvant-free MUC1 Glycopeptide Vaccine for Cancer Therapy. J Am Chem Soc. 2012; 134:8730–8733. [PubMed: 22587010]
48. Schietinger A, Philip M, Yoshida BA, Azadi P, Liu H, Meredith SC, Schreiber H. A mutant Chaperone Converts a Wild-type Protein into a Tumor-Specific Antigen. Science. 2006; 314:304–308. [PubMed: 17038624]
49. Wang Y, Ju T, Ding X, Xia B, Wang W, Xia L, He M, Cummings RD. Cosmc is An Essential Chaperone for Correct Protein O-Glycosylation. Proc Natl Acad Sci U S A. 2010; 107:9228–9233. [PubMed: 20439703]
50. Brinas RP, Sundgren A, Sahoo P, Morey S, Rittenhouse-Olson K, Wilding GE, Deng W, Barchi JJ. Design and Synthesis of Multifunctional Gold Nanoparticles Bearing Tumor-Associated Glycopeptide Antigens as Potential Cancer Vaccines. Bioconjugate Chem. 2012; 23:1513–1523.
51. Yin Z, Comellas-Aragones M, Chowdhury S, Bentley P, Kaczanowska K, BenMohamed L, Gildersleeve JC, Finn MG, Huang X. Boosting Immunity to Small Tumor-Associated Carbohydrates with Bacteriophage Qβ capsids. ACS Chem Biol. 2013; 8:1253–1262. [PubMed: 23505965]
52. Parry AL, Clemson NA, Ellis J, Bernhard SSR, Davis BG, Cameron NR. 'Mulicopy Multivalent' Glycopolymer-Stabilized Gold Nanoparticles as Potential Synthetic Cancer Vaccines. J Am Chem Soc. 2013; 135:9362–9365. [PubMed: 23763610]
53. Newman KD, Sosnowski DL, Kwon GS, Samuel J. Delivery of MUC1Mucin Peptide by Poly(D,L-Lactic-co-Glycolic Acid) Microspheres Induces Type 1 T Helper Immune Responses. J Pharm Sci. 1998; 87:1421–1427. [PubMed: 9811500]
54. Ojeda R, de Paz JL, Barrientos AG, Martin-Lomas M, Penades S. Preparation of Multifunctional Glyconanoparticles As A Platform for Potential Carbohydrate-Based Anticancer Vaccines. Carbohydr Res. 2007; 342:448–59. [PubMed: 17173881]
55. Kinarsky L, Suryanarayanan G, Prakash O, Paulsen J, Clausen H, Hanisch FA, Hollingsworth MA, Sherman S. Conformational Studies on the MUC1 Tandem Repeat Glycopeptides: Implication for the Enzymatic O-Glycosylation of the Mucin Protein Core. Glycobiology. 2003; 13:929–939. [PubMed: 12925576]
56. Karsten U, Serttas N, Paulsen H, Danielczyk A, Goletz S. Binding Patterns of DTR-Specific Antibodies Reveal a Glycosylation-Conditioned Tumor-Specific Epitope of the Epithelial Mucin (MUC1). Glycobiology. 2004; 14:681–692. [PubMed: 15115750]
57. Matsushita T, Ohyabu N, Fujitani N, Naruchi K, Shimizu H, Hinou H, Nishimura S. Site-Specific Conformational Alteration Induced by Sialylation of MUC1 Tandem Repeating Glycopeptides at An Epitope Region for the Anti-KL-6 Monoclonal Antibody. Biochemistry. 2013; 52:402–414. [PubMed: 23259747]

58. Ryan SO, Turner MS, Gariepy J, Finn OJ. Tumor Antigen Epitopes Interpreted by the Immune System as Self or Abnormal-Self Differentially Affect Cancer Vaccine Responses. Cancer Res. 2010; 70:5788–5796. [PubMed: 20587526]

59. Burford B, Gentry-Maharaj A, Graham R, Allen D, Pedersen JW, Nudelman AS, Blixt O, Fourkala EO, Bueti D, Dawnay A, Ford J, Desai R, David L, Trinder P, Acres B, Schwientek T, Gammerman A, Reis CA, Silva L, Osorio H, Hallett R, Wandall HH, Mandel U, Hollingsworth MA, Jacobs I, Fentiman I, Clausen H, Taylor-Papadimitriou J, Menon U, Burchell JM. Autoantibodies to MUC1 Glycopeptides Cannot Be Used as A Screening Assay for Early Detection of Breast, Ovarian, Lung or Pancreatic Cancer. Br J Cancer. 2013; 108:2045–2055. [PubMed: 23652307]

60. Tarp MA, Sorensen AL, Mandel U, Paulsen H, Burchell J, Taylor-Papadimitriou J, Clausen H. Identification of A Novel Cancer-Specific Immunodominant Glycopeptide Epitope in the MUC1 Tandem Repeat. Glycobiology. 2006; 17:197–209. [PubMed: 17050588]

61. Sorensen AL, Reis CA, Tarp MA, Mandel U, Ramachandran K, Sankaranarayanan V, Schwientek T, Graham R, Taylor-Papadimitriou J, Hollingsworth MA, Burchell J, Clausen H. Chemoenzymatically Synthesized Multimeric Tn/STn MUC1 Glycopeptides Elicit Cancer-Specific Anti-MUC1 Antibody Responses and Override Tolerance. Glycobiology. 2006; 16:96–107. [PubMed: 16207894]

62. Brockhausen I. Mucin-type O-glycans in human colon and breast cancer: glycodynamics and functions. EMBO Rep. 2006; 7:599–604. [PubMed: 16741504]

63. Muller S, Hanisch FG. Recombinant MUC1 Probe Authentically Reflects Cell-Specific O-glycosylation Profiles of Endogenous Breast Cancer Mucin. High Density and Prevalent Core 2-based Glycosylation. J Biol Chem. 2002; 277:26103–26112. [PubMed: 12000758]

64. Westerlind U, Hobel A, Gaidzik N, Schmitt E, Kunz H. Synthetic Vaccines Consisting of Tumor-Associated MUC1 Glycopeptide Antigens and A T-cell Epitope for the Induction of A Highly Specific Humoral Immune Response. Angew Chem, Int Ed. 2008; 47:7551–7556.

65. Cai H, Sun ZY, Huang ZH, Shi L, Zhao YF, Kunz H, Li YM. Fully Synthetic Self-Adjuvanting Thioether-Conjugated Glycopeptide-Lipopeptide Antitumor Vaccines for the Induction of Complement-Dependent Cytotoxicity Against Tumor Cells. Chem - Eur J. 2013; 19:1962–1970. [PubMed: 23280874]

66. Gaidzik N, Westerlind U, Kunz H. The development of synthetic antitumour vaccines from mucin glycopeptide antigens. Chem Soc Rev. 2013; 42:4421–4442. [PubMed: 23440054]

67. Backstrom M, Link T, Olson FJ, Karlsson H, Graham R, Picco G, Burchell J, Taylor-Papadimitriou J, Noll T, Hansson GC. Recombinant MUC1Mucin with A Breast Cancer-like O-Glycosylation Produced in Large Amounts in Chinese-Hamster Ovary Cells. Biochem J. 2003; 376:677–686. [PubMed: 12950230]

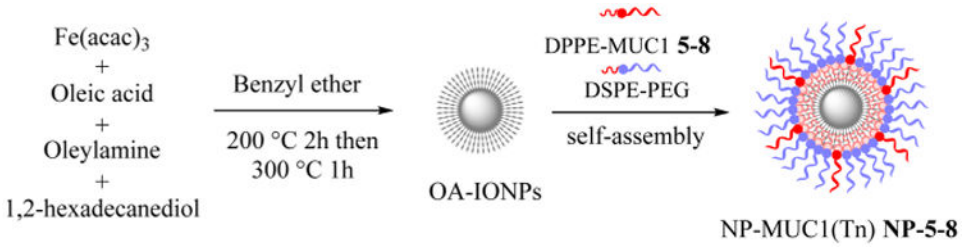

Figure 1.

Synthesis of hydrophobic OA-IONPs by the thermal decomposition method and monolayer self-assembly coating of the NPs by phospholipid-functionalized MUC1 or MUC1(Tn) glycopeptide.

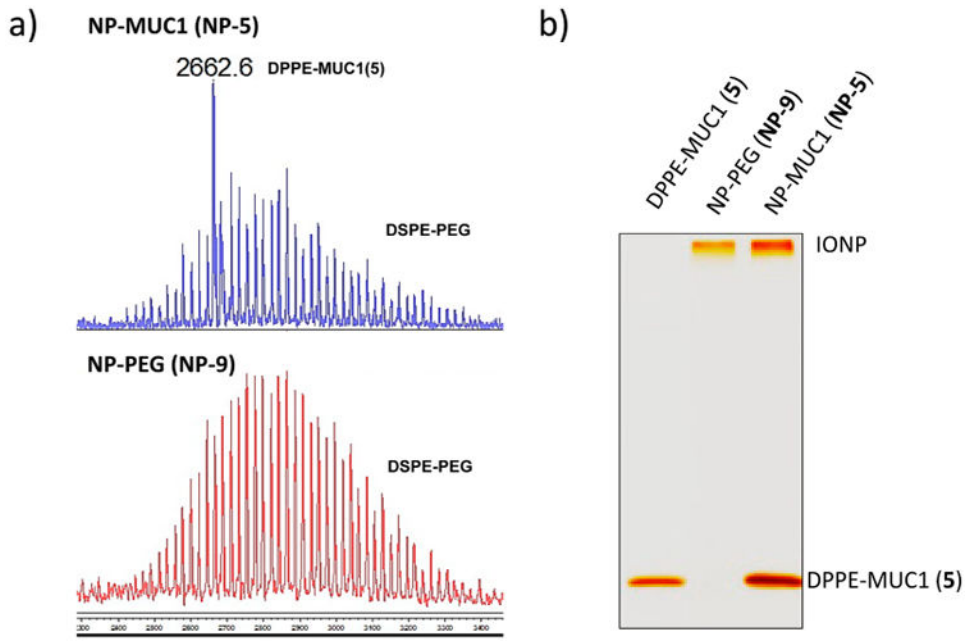

Figure 2.

(a) MALDI-TOF mass spectrum of **NP-5** coated with lipopeptide **5** ($[M + H]^+ = 2662$) and DSPE-PEG (top spectrum) and **NP-9** coated with DSPE-PEG only (bottom spectrum). (b) SDS-PAGE of DPPE-MUC1, NP-PEG (**NP-9**), and NP-MUC1 (**NP-5**). The gel was visualized through silver staining.

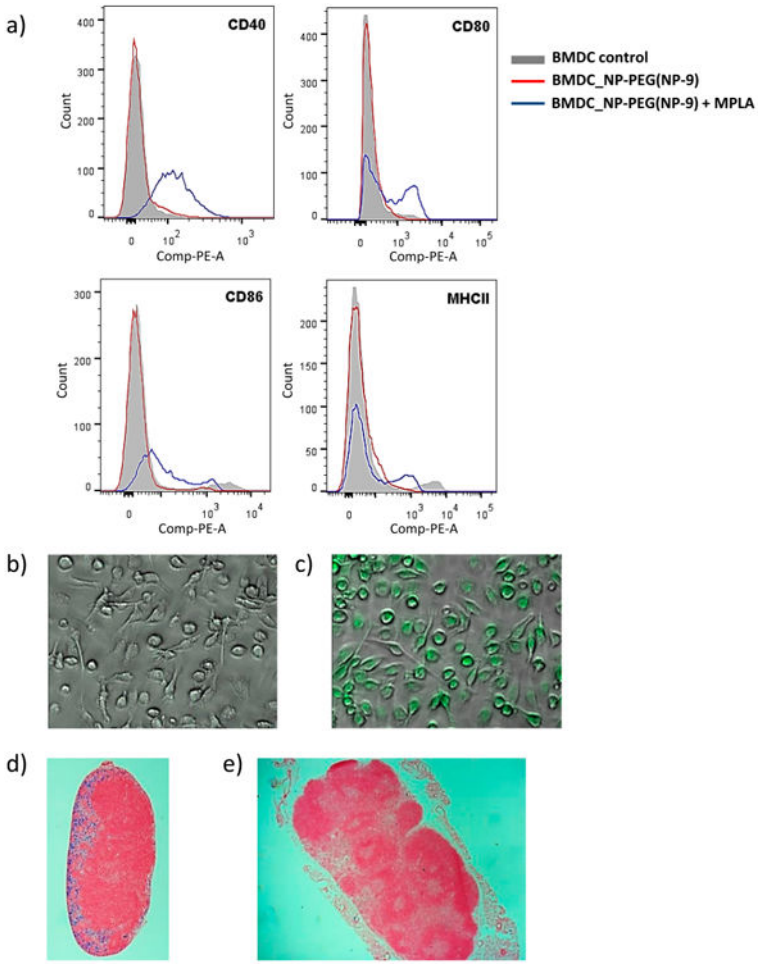

Figure 3.

(a) Flow cytometry results showing the expression of cellular markers of the activation state of BMDCs (CD40, CD80, CD86, and MHCII) after incubation with NP-PEG (**NP-9**) (red line) or NP-PEG (**NP-9**) + MPLA (blue line). Confocal images of BMDCs incubated with (b) PBS and (c) **NP-9** (FITC) + MPLA. Histology of sections of an (d) axillary (local) lymph node and (e) inguinal (distant) lymph node stained by Prussian blue.

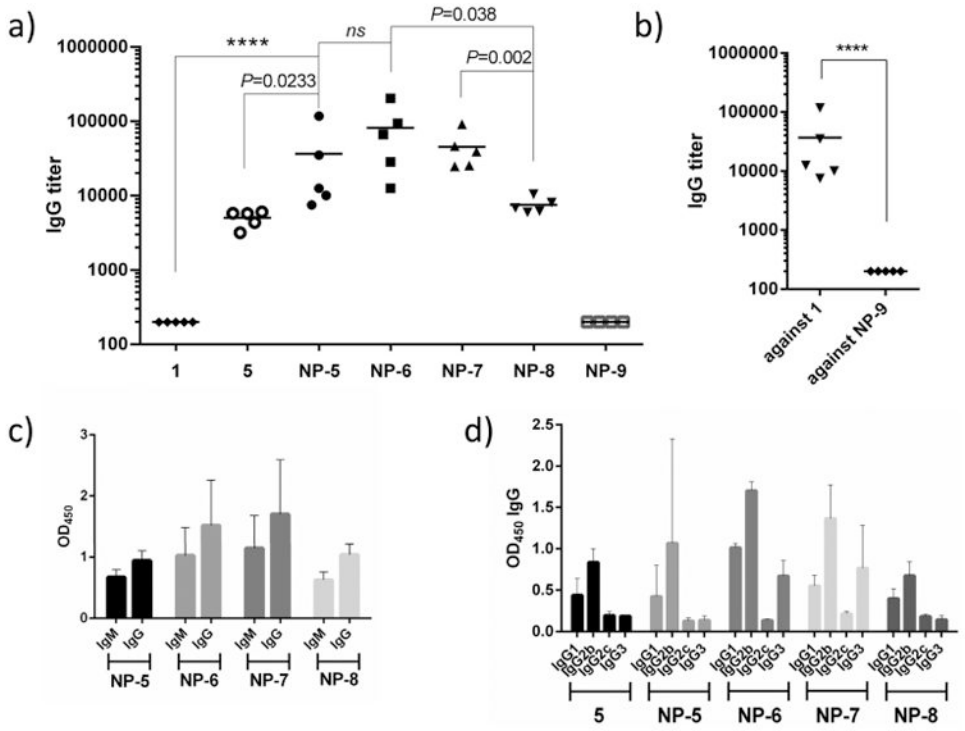

Figure 4.

(a) Anti-MUC1 and anti-Tn-MUC1 antibody titers from individual mice (n = 5) collected on day 35 after immunization with NP-MUC1 (**NP-5**) and NP-MUC1(Tn) (**NP-6**, **NP-7**, and **NP-8**) vaccines compared with those of mice immunized with soluble MUC1 peptide **1** and lipo-MUC1-peptide **5**. The anti-MUC1 antibody titers were determined by an ELISA coated with corresponding (glyco)peptides **1–4**. (b) IgG antibody titers from individual mice collected on day 35 after immunization with NP-MUC1 (**NP-5**) against MUC1 peptide **1** and **NP-9**. (c) IgM/IgG antibody response determined by ELISA at a 3200-fold dilution of serum from mice immunized with different vaccines. (d) IgG isotypes of antibody response determined by ELISA from mice immunized with various vaccines.

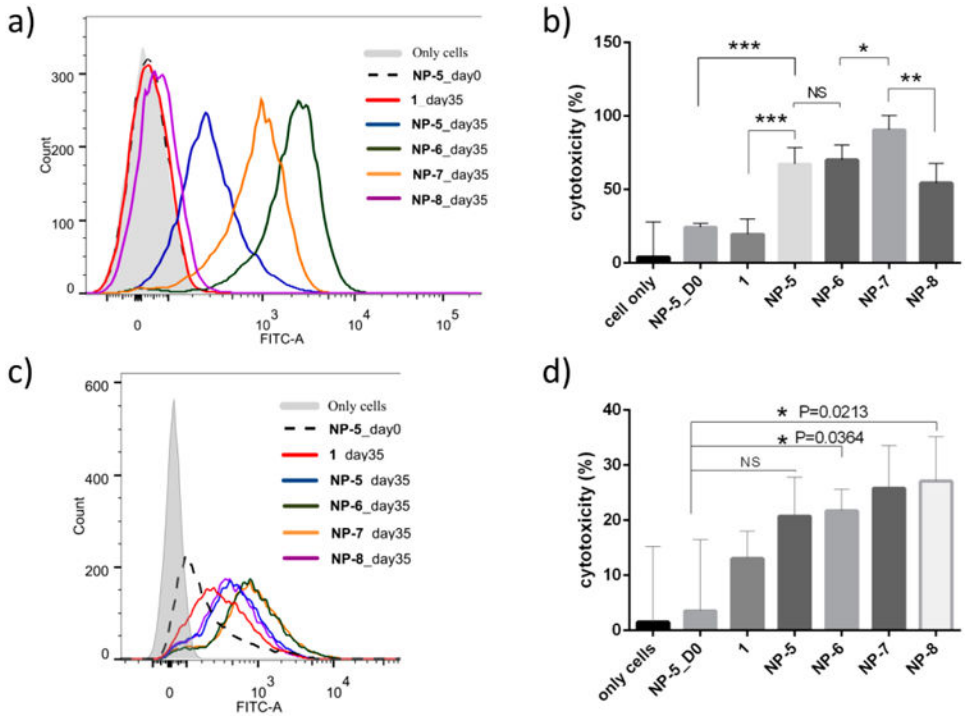

Figure 5.

Flow cytometric analysis of the binding of antibodies induced by various constructs to (a) MUC1-Ag104 cells and (c) MCF-7. MTS assay analysis of complement-dependent cytotoxicity of antibodies induced by various vaccines on (b) MUC1-Ag104 cells and (d) MCF-7 (**, $P < 0.05$; ***, $P < 0.005$).

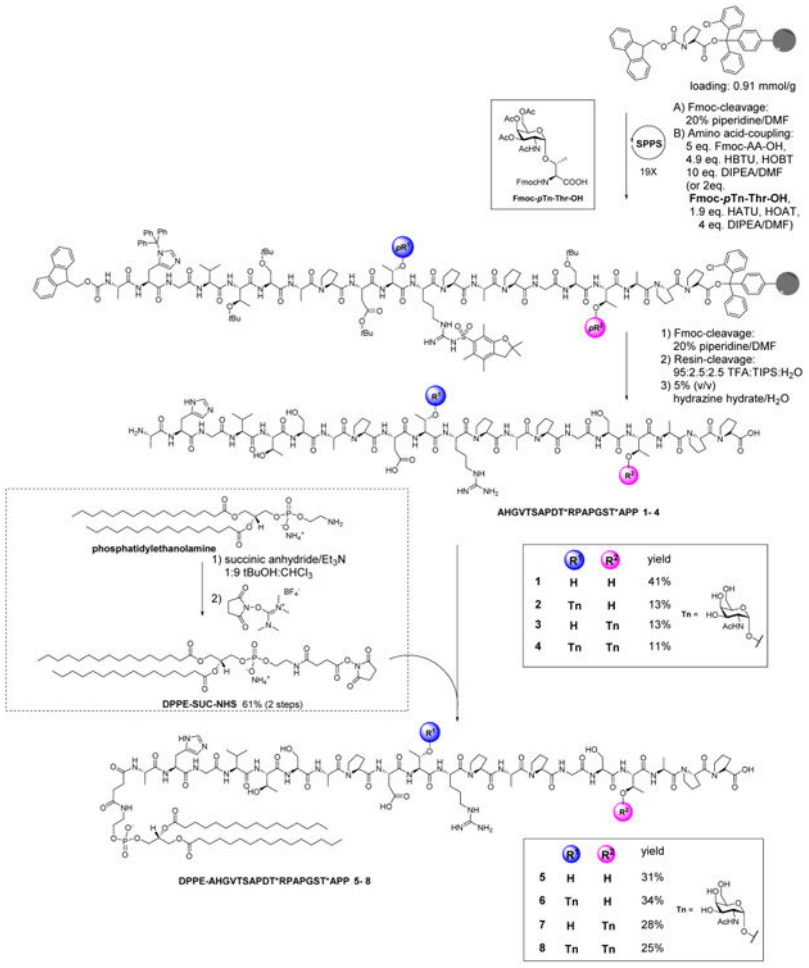

Scheme 1. Synthesis of MUC1 Lipo-(glyco)peptides[a]

[a](Tn-)MUC1 peptides **1–4** were synthesized by solid-phase peptide synthesis followed by coupling with the activated phospholipid, **DPPE-SUC-NHS**, to yield MUC1 lipo-(glyco)peptides **5–8**.

Table 1

Hydrodynamic Sizes and Zeta Potentials of the NP Vaccines in PBS

NP	size [nm]	PDI	zeta [mV]
NP-PEG (**NP-9**)	31.8	0.257	−2.53
NP-5	32.2	0.294	−2.86
NP-6	37.6	0.288	−1.83
NP-7	38.1	0.265	−2.94
NP-8	38.4	0.269	−2.37